Machine Learning Based Predictions of Airfoil Aerodynamic Coefficients for Reynolds Number Extrapolations

Machine Learning Based Predictions of Airfoil Aerodynamic Coefficients for Reynolds Number Extrapolations

Ahmet Can ÖZGÖREN[1,2], Deniz Alper ACAR[2], Recep KAMRAK[1], Görkem Mahir ERİŞ[1], Yasin ÖZDEMİR[1], Nilay Sezer UZOL[1,3], Oğuz UZOL[1,3]

[1] Department of Aerospace Engineering, Middle East Technical University (METU), Ankara, Turkey
[2] HAVELSAN Inc., Ankara, Turkey
[3] METU Center for Wind Energy Research (RÜZGEM), Ankara, Turkey

Corresponding Author: Oguz Uzol, uzol@metu.edu.tr

Abstract. This study investigates the application of various machine learning (ML) algorithms for predicting two critical aerodynamic coefficients, i.e. the maximum lift coefficient ($C_{l\,max}$) and the minimum drag coefficient ($C_{d\,min}$), for wind turbine airfoils at any given Reynolds number. We propose to use clustering techniques to group similar airfoil shapes and use the created partitions to predict unseen airfoil properties utilizing their similarity. Here, we also represent airfoils in the PARSEC low dimensional space, rather than high dimensional airfoil points space, to remedy the small number of training data. For this purpose, an extended experimental airfoil database is created and used for training models based on five different ML algorithms. We observe that the Decision Tree Ensemble (DTE), Random Forest (RF) and multi-layer perceptron (MLP) models emerge as the most effective predictors for $C_{l\,max}$ and $C_{d\,min}$. Testing these two ML models on three additional airfoil cases not included in the training database shows that the $C_{l\,max}$ prediction performance is generally reasonable, with error levels being around 5% on average. In contrast, the prediction error levels for $C_{d\,min}$ are usually higher, with an average of around 15%.

1. Introduction

Aerodynamic design as well as performance analysis of a wind turbine blade heavily relies on Blade Element Momentum (BEM) theory-based fast analysis tools, which in turn rely on accurate aerodynamic coefficient data (i.e., airfoil polars) for the airfoils used in the blade design.

These airfoil polars can either be generated numerically or through wind tunnel tests. When available, experimentally obtained polars are preferred in general since numerical tools could have difficulty in predicting aerodynamic characteristics, especially the maximum lift coefficient ($C_{l\,max}$), minimum drag coefficient ($C_{d\,min}$) and stall angle (α_{stall})[1]. Note that experimental data of course will have measurement uncertainties and variations between different facilities may be observed, however these variations are generally limited and the data in general are more reliable than simulation results, especially for the two aerodynamic coefficients considered in this study, i.e. $C_{l\,max}$ and $C_{d\,min}$[2]. In a typical industrial wind tunnel campaign, these data are generally obtained at relatively lower Reynolds numbers compared to the ones observed in real operational conditions. The measured aerodynamic data then have to be extrapolated to higher Reynolds numbers in order to be used in blade design.

Though scarce, some methodologies have been proposed over the years for Reynolds number extrapolation. Yamauchi and Johnson[3] proposed a power-law-based referencing equation to extrapolate Reynolds number effects on $C_{l\,max}$ and $C_{d\,min}$ for helicopter airfoil applications. Similarly, Peterson and Rizzi[4] developed a methodology to scale $C_{d\,min}$ for airfoils used in fixed-wing aeroplanes, suggesting a range of power coefficients based on Prandtl's analysis. In another effort for wind turbine airfoils, Ceyhan[5] proposed to calculate trends from RFOIL and CFD simulations to predict high Reynolds number effects. Recently, Özgören and Uzol[6,7] proposed a data-driven extrapolation methodology to first predict $C_{l\,max}$, $C_{d\,min}$ and α_{stall} using generated response surfaces based on an experimental airfoil database and then to predict full airfoil polars through a power-law type implementation.

In recent years, data-driven techniques have become increasingly popular, and machine learning algorithms are being implemented in a variety of aerodynamics problems[8,9]. In this context, this study will investigate the prediction performance of different machine learning algorithms to predict $C_{l\,max}$ and $C_{d\,min}$, at any given Reynolds number as an extension of the more statistical and response-surface based prediction technique described in Özgören and Uzol[6,7]. The models are trained using an expanded version of the experimental airfoil database in Özgören and Uzol[6,7], which is constructed from available data in open literature. The predicted $C_{l\,max}$ and $C_{d\,min}$ values at high Reynolds numbers can then be used to obtain full polars using the methodology described in Özgören and Uzol[6,7].

2. Methodology

2.1. The Airfoil Aerodynamic Coefficient Database

The experimental database consists of 128 different airfoil profiles with measured aerodynamic data in a Reynolds number range between $1x10^6$ and $9x10^6$ (392 experimental data in total). Most of these are NACA airfoils, and a digitized version is available in open literature[10]. Additionally, a limited number of airfoils commonly used in wind turbine applications have also been added to the database. A complete list of the included airfoils in the database is given in Table 1.

Table 1. Airfoil database used in this study with experimentally obtained aerodynamic coefficients.

NACA0006	$NACA63_{(2)}415$	NACA65,3-618	NACA66-006
NACA0009	$NACA63_{(2)}615$	$NACA65_{(216)}$-415,a=0.5	NACA66-009
NACA1408	$NACA63_{(3)}218$	NACA65-006	NACA66-206
NACA1410	$NACA63_{(3)}418$	NACA65-009	NACA66-209
NACA1412	$NACA63_{(3)}618$	NACA65-206	NACA66-210
NACA2412	$NACA63_{(4)}021$	NACA65-209	$NACA66_{(1)}012$
NACA2415	$NACA63_{(4)}221$	NACA65-210	$NACA66_{(1)}212$
NACA2418	$NACA63_{(4)}421$	NACA65-410	$NACA66_{(2)}015$
NACA2421	NACA64-006	$NACA65_{(1)}012$	$NACA66_{(2)}215$
NACA2424	NACA64-009	$NACA65_{(1)}212$	$NACA66_{(2)}415$
NACA4412	NACA64-108	$NACA65_{(1)}212$,a=0,6	$NACA66_{(3)}018$
NACA4415	NACA64-110	$NACA65_{(1)}412$	$NACA66_{(3)}218$
NACA4418	NACA64-206	$NACA65_{(2)}015$	$NACA66_{(3)}418$
NACA4421	NACA64-208	$NACA65_{(2)}215$	$NACA66_{(4)}021$
NACA4424	NACA64-209	$NACA65_{(2)}415$	$NACA66_{(4)}221$
NACA23012	NACA64-210	$NACA65_{(2)}$-415,a=0.5	NACA67,1-215
NACA23015	$NACA64_{(1)}012$	$NACA65_{(3)}018$	NACA747A315
NACA23018	$NACA64_{(1)}112$	$NACA65_{(3)}218$	NACA747A415
NACA23021	$NACA64_{(1)}212$	$NACA65_{(3)}418$	AH93-W-257

NACA23024	NACA64$_{(1)}$412	NACA65$_{(3)}$-418,a=0.5	AH93-W-300
NACA63$_{(420)}$-442	NACA64$_{(2)}$015	NACA65$_{(3)}$-618,a=0.5	AH94-W301
NACA63$_{(420)}$-517	NACA64$_{(2)}$215	NACA65$_{(4)}$021	DU91-W2-250
NACA63-006	NACA64$_{(2)}$415	NACA65$_{(4)}$221	DU93-W-210
NACA63-009	NACA64$_{(3)}$018	NACA65$_{(4)}$421	DU97-W-300
NACA63-206	NACA64$_{(3)}$218	NACA65$_{(4)}$-421,a=0.5	FFA-W3-211
NACA63-209	NACA64$_{(3)}$418	NACA65$_{(215)}$114	FFA-W3-241
NACA63-210	NACA64$_{(3)}$618	NACA65($_{421)}$420	FFA-W3-301
NACA63$_{(1)}$012	NACA64$_{(4)}$021	NACA66,1-212	FX66-S196-V1
NACA63$_{(1)}$212	NACA64$_{(4)}$221	NACA66$_{(215)}$016	S814
NACA63$_{(1)}$412	NACA64$_{(4)}$421	NACA66$_{(215)}$216	S825
NACA63$_{(2)}$015	NACA65,3-018	NACA66$_{(215)}$216,a=0.6	S827
NACA63$_{(2)}$215	NACA65,3-418,a=0.8	NACA66$_{(215)}$416	S809

2.2. The Airfoil Geometry Parameterization

Given the limited number of data points, reducing the dimensionality of the input domain would significantly improve training of the machine learning models. Each airfoil geometry included in the database is parameterized using the PARSEC airfoil parameterization methodology[11]. This methodology is based on 12 geometrically meaningful parameters to express the airfoil geometry[12]. These PARSEC parameters, given in Figure 1, are used as inputs in the machine learning algorithms. We can treat the 12-dimensional space parameterized by PARSEC as the latent variable in a larger auto-encoder model, where airfoil points serve as input/output. Essentially, this mapping enables training a smaller and shallower model using the scarce available data. Using PARSEC, we bypass the initial layers that would have been there to map the large number of points in airfoil shape to a lower dimensional space and make the model focus on learning the underlying mapping between our low dimensional inputs and our output.

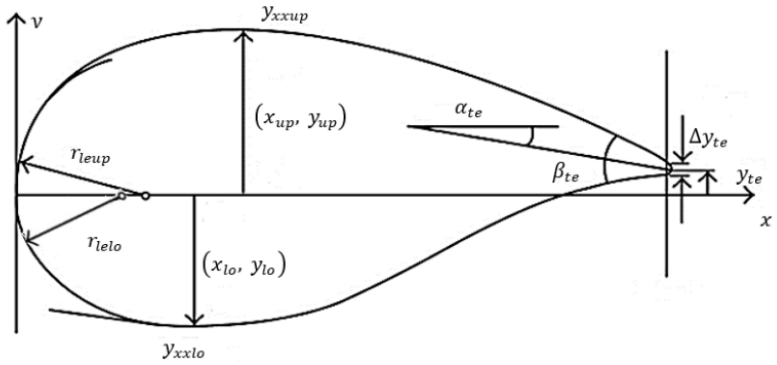

Figure 1. PARSEC parameters for an airfoil profile[11]

2.3. Machine Learning Algorithms

The airfoil aerodynamic database is then used to train machine learning models using various algorithms. The 12 PARSEC parameters and the Reynolds number are inputs, and $C_{l\,max}$ and $C_{d\,min}$ are outputs. This scheme is illustrated in Figure 2. In this study, we investigate five different algorithms, which are the Linear Regression Model (LRM), Support Vector Machines (SVM), Decision Tree Ensemble (DTE), Random Forest (RF) and Multi Layer Perceptron (MLP) [13,14].

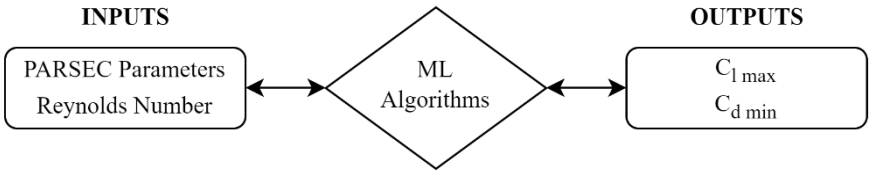

Figure 2. The scheme used for training the database.

Airfoil shapes play a crucial role in determining aerodynamic performance. It is widely observed that similar airfoil geometries exhibit similar aerodynamic characteristics. Building upon this insight, our research investigates the performance of the clustering methods within a regression framework to predict aerodynamic coefficients. Specifically, we aim to predict airfoil characteristics based on existing measurement data by clustering similar airfoils closer together and dissimilar airfoils farther apart. Also, while airfoil characteristics typically exhibit a non-linear relationship with their shape, in numerous instances a linear correlation exists between the airfoil shape parameters and their associated characteristics (for instance Sadraey[15] suggests a linear relationship between lift curve slope and airfoil maximum thickness). Hence, this work compares classification-based results with results obtained by Multi Layer Perceptron (MLP) feedforward neural nets and with linear regression models. The goal is to identify the most effective approach for predicting $C_{l\,max}$ and $C_{d\,min}$.

2.4. Training Procedure

In this study, the test dataset is fixed and thus excluded from the training and cross-validation process, which are the sole focus of this paper. The training data is partitioned into an 90-10 split for training and cross-validation, respectively. The scaling for the PARSEC parameters was set to value 1 whereas the scaling for the Re was set to $8x10^6$. The outputs were scaled by the min-max scaling method.

We explored a vast array of MLP architectures on this dataset, ultimately selecting a model with a neuron configuration of 1024, 128, and 128. This model employs a LeakyReLU activation function with a negative slope coefficient of 0.2 and has demonstrated superior performance on cross-validation data. Given the modest size of the dataset, the batch size was set to be equal to the entirety of the training data, and each model underwent training for up to one hundred thousand epochs on CUDA 1080 Ti GPUs. The learning rate was treated as a variable during the architecture search, tested at 0.1, 0.01, and 0.001, with the final model being trained at a learning rate of 0.001. For optimization, the ADAM optimizer was employed, adhering to the default beta parameters of PyTorch (Beta1 = 0.9 and Beta2 = 0.999). To ensure robustness, the training data was shuffled prior to each forward pass of the MLP models.

During the training of the Random Forest (RF) model, Least-Squares Boosting (LSBoost) was applied for various numbers of regression trees and the model with 150 regression trees was selected. For the training of the Decision Tree Ensemble (DTE), the bagging ensemble method was applied for the same number of regression trees selected for random forest for each model. This was done in order to be able to compare the results of DTE and RF. Lastly for training the SVM model the gaussian kernel was used.

3. Results

3.1. Performance of the Machine Learning Models

The constructed airfoil experimental database is used in the training of the models using five different algorithms that are explained in Section 2.3. These models are then used to predict $C_{l\,max}$ and $C_{d\,min}$ values using the airfoil PARSEC parameters and the required Reynolds number as inputs to the models.

Here two performance metrics are investigated for each model. The first tries to assess the capacity of each model in learning the underlying mapping from inputs to outputs. The second tries to assess the performance of each model when predicting the $C_{l\,max}$ and $C_{d\,min}$ values for a set of test airfoils for

which some are similar to the ones used in training and some are dissimilar to the training data. For these airfoils, we also investigate the prediction performance of the models for Re numbers that are never seen by the model.

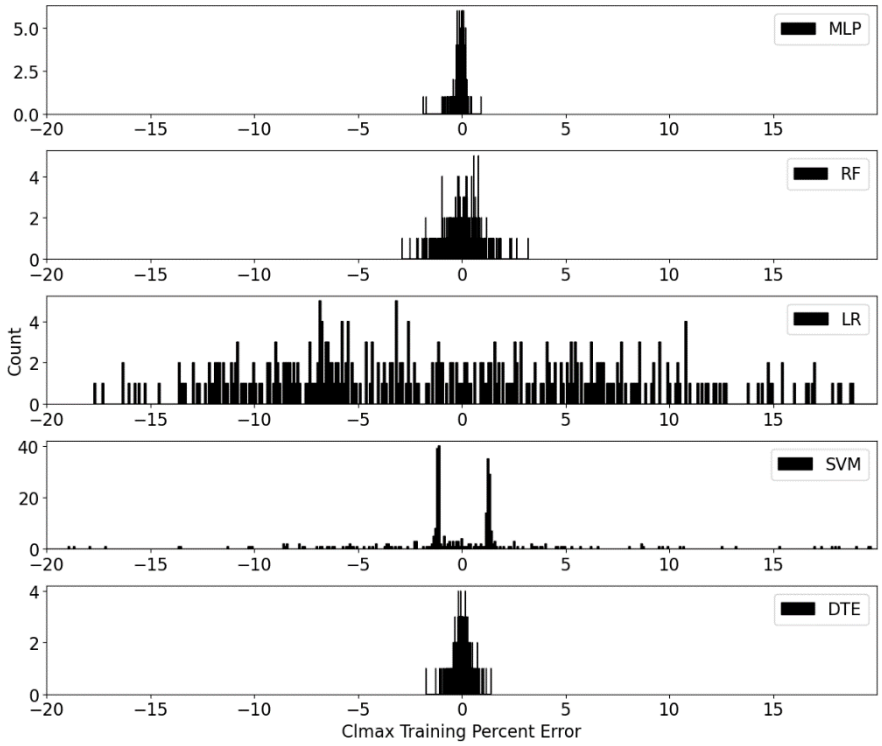

Figure 3. Error percentage distributions for $C_{l\,max}$ for the trained ML models. MLP: Multi Layer Perceptron, RF: Random Forest, LR: Linear Regression Model, SVM: Support Vector Machines, DTE: Decision Tree Ensemble

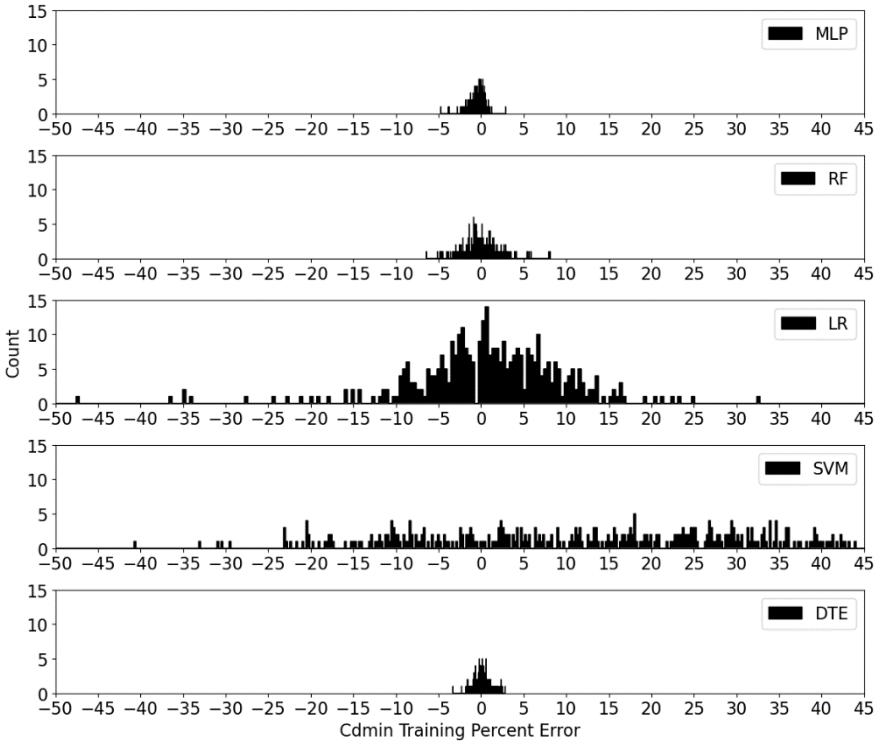

Figure 4. Error percentage distributions for $C_{d\,min}$ for the trained ML models. MLP: Multi Layer Perceptron, RF: Random Forest, LR: Linear Regression Model, SVM: Support Vector Machines, DTE: Decision Tree Ensemble

Figures 3 and 4 illustrate the training capacity of each model as a histogram of their respective errors on training data, after the training process for each model is concluded. This capacity is measured by the capability of the model to minimize the error for predicting the training data. Here, we tried to select models that minimize the mean squared error MSE. As to eliminate the possibility of overfitting, the limit for the MSE of an epoch is set to $1x10^{-6}$.

The linear regression was employed here to investigate if any simple relationship may be observed after training the model. For LR, new non-linear features were created by combinations of inputs up to their third degree. Yet, the model did not perform well as expected on the training data. The performance of the SVM model was lacking on the training data as a hyperplane might not be enough for clustering the complex airfoil shapes into two categories based on their aerodynamics characteristics. Due to the unsatisfactory performance of these two models, their results are not included at Tables 2 and 3, which are presented later in this paper.

We also observe that the same models perform better in learning the $C_{l\,max}$ than $C_{d\,min}$. The reason for that might be due to the measurement error percentage inherent in experimental data. In other words, the measurement errors (for the same error bounds) will affect the $C_{d\,min}$ measurements and their distribution more as $C_{d\,min}$ values are generally two to three orders of magnitude smaller than $C_{l\,max}$ values. Due to this fact, the uncertainty in the measurements of the $C_{d\,min}$ are two to three orders higher than that of the $C_{l\,max}$ which also in turn affects the prediction error bounds of models trained on each coefficient. In addition, regarding the learning/overfitting capacity of the selected models, when compared in terms of flexibility the MLP is the most flexible model and then comes the DTE and RF models, respectively. The same flexibility is observed in Figures 3 and 4 when comparing the standard deviation levels.

3.2. Prediction Results for Test Airfoilss

Three different airfoils, i.e. NACA65$_{(3)}$618, DU00-W-212 and NACA63$_{(3)}$018, are selected as test airfoils, and are not included in the training process to test the prediction performance of the trained models.

Table 2. Comparison of $C_{l\,max}$ predictions with experimental data for test airfoils

Airfoil Name	Reynolds Number [x10^{-6}]	Experimental	RF Predicted (Error %)	DTE Predicted (Error %)	MLP Predicted (Error %)
NACA65$_{(3)}$618	3	1.41	1.36 (-3.5)	1.36 (-3.5)	1.38 (-2.1)
NACA65$_{(3)}$618	6	1.55	1.52 (-1.9)	1.51 (-2.6)	1.52 (-1.9)
NACA65$_{(3)}$618	9	1.65	1.61 (-2.4)	1.61 (-2.4)	1.62 (-1.8)
DU00-W-212	3	1.29	1.44 (11.6)	1.43 (10.9)	1.39 (7.8)
DU00-W-212	6	1.46	1.42 (-2.7)	1.42 (-2.7)	1.49 (2.1)
DU00-W-212	9	1.56	1.53 (-1.9)	1.53 (-1.9)	1.51 (-3.2)
DU00-W-212	12	1.63	1.53 (-6.1)	1.53 (-6.1)	1.53 (-6.1)
DU00-W-212	15	1.66	1.53 (-7.8)	1.53 (-7.8)	1.48 (-10.8)
NACA63$_{(3)}$018	3	1.26	1.23 (-2.4)	1.23 (-2.4)	1.30 (3.2)
NACA63$_{(3)}$018	6	1.45	1.38 (-4.8)	1.38 (-4.8)	1.42 (-2.1)
NACA63$_{(3)}$018	9	1.52	1.52 (0.0)	1.52 (0.0)	1.49 (-2.0)
NACA63$_{(3)}$018	15	1.63	1.52 (-6.7)	1.52 (-6.7)	1.45 (-11.0)
NACA63$_{(3)}$018	20	1.64	1.52 (-7.3)	1.52 (-7.3)	1.45 (-11.6)

Table 3. Comparison of $C_{d\,min}$ predictions with experimental data for test cases

Airfoil Name	Reynolds Number [x10^{-6}]	Experimental	RF Predicted (Error %)	DTE Predicted (Error %)	MLP Predicted (Error %)
NACA65$_{(3)}$618	3	0.005520	0.006055 (9.7)	0.006122 (10.9)	0.005428 (-1.7)
NACA65$_{(3)}$618	6	0.004770	0.005234 (9.7)	0.005234 (9.7)	0.004468 (-6.3)
NACA65$_{(3)}$618	9	0.004320	0.005061 (17.2)	0.005056 (17.0)	0.004298 (-0.5)
DU00-W-212	3	0.007000	0.005415 (-22.6)	0.00540 (-22.9)	0.006500 (-7.1)
DU00-W-212	6	0.006010	0.004392 (-26.9)	0.004466 (-25.7)	0.005940 (-1.2)
DU00-W-212	9	0.005660	0.004120 (-27.2)	0.004091 (-27.7)	0.005882 (3.9)
DU00-W-212	12	0.005580	0.004120 (-26.2)	0.004091 (-26.7)	0.005806 (4.1)
DU00-W-212	15	0.005480	0.004120 (-24.8)	0.004091 (-25.3)	0.006287 (14.7)
NACA63$_{(3)}$018	3	0.005835	0.005998 (2.8)	0.006050 (3.7)	0.005775 (-1.0)
NACA63$_{(3)}$018	6	0.005311	0.004856 (-8.6)	0.004850 (-8.7)	0.005200 (-2.1)
NACA63$_{(3)}$018	9	0.005013	0.004661 (-7.0)	0.004715 (-5.9)	0.004823 (-3.8)
NACA63$_{(3)}$018	15	0.004785	0.004661 (-2.6)	0.004715 (-1.5)	0.005092 (6.4)
NACA63$_{(3)}$018	20	0.005262	0.004661 (-11.4)	0.004715 (-10.4)	0.005772 (9.7)

As the constructed airfoil database primarily comprises of NACA airfoil profiles, it is crucial to assess the prediction performance for a NACA profile. Due to this reason, NACA65$_{(3)}$618 airfoil is selected as one of the test airfoils. Polar data of this airfoil is available at Reynolds numbers 3x10^6, 6x10^6 and 9x10^6. The other test airfoil, DU00-W-212, was previously experimentally tested in the DNW-HDG wind tunnel at 3x10^6, 6x10^6, 9x10^6, 12x10^6 and 15x10^6 Reynolds numbers within the context of the AVATAR project[16]. The last test airfoil is the symmetrical NACA63$_{(3)}$018 airfoil for which the aerodynamic polar data are available at 3x10^6, 6x10^6, 9x10^6, 15x10^6 and 20x10^6. Tables 2 and 3 present the results regarding the prediction performance of the top three models, i.e. Random Forest (RF), Decision Tree Ensemble (DTE) and Multilayer Perceptron (MLP).

Regarding $C_{l\,max}$ predictions for the test airfoils, results presented in Table 2 show that even though these airfoils are not included in the training database the error levels are generally below 12% and the average error for all cases is 4.5%. For $C_{d\,min}$ predictions, the error levels are generally higher compared to those of $C_{l\,max}$ predictions (error levels as high as 27% are observed) with an average error level of

about 15%. Both for $C_{l\,max}$ and $C_{d\,min}$ predictions and for all cases with a Reynolds number higher than $9x10^6$, we observe that the predicted values are all similar (with some improvements in the case of MLP) for three ML models. The improvement in the results of MLP can be attributed to its higher capacity to learn compared to the other models. Yet, during architecture search it was observed that the MLP is more susceptible to overfitting compared to other models. With a larger number of parameters, the MLP shows promising results even for the airfoils that are dissimilar to the ones it is trained on and Reynolds numbers that are out of bound for its training data.

4. Conclusions

In this paper, we have presented machine learning (ML) based methods to predict aerodynamic coefficients, i.e. $C_{l\,max}$ and $C_{d\,min}$, to be used in Reynolds number extrapolation methods previously proposed in the literature. For this purpose, an airfoil database of experimentally obtained aerodynamic data has been utilized to train ML models using five different machine learning algorithms. It is observed that the Decision Tree Ensemble (DTE), Random Forest (RF) and Multi Layer Perceptron (MLP) models show better performance in general in terms of $C_{l\,max}$ and $C_{d\,min}$ prediction capability. Testing these three ML models on three additional airfoil cases that are not included in the training database show that the $C_{l\,max}$ prediction performance is reasonable in general with error levels being around 5% in average, while the prediction error levels for $C_{d\,min}$ are generally higher with an average around 15%. This higher error rate for the $C_{d\,min}$ is attributed to the fact that the scale of the minimum drag coefficient is two to three orders of magnitude smaller than the maximum lift coefficient and thus will be more affected by the measurement errors. This can also be observed when investigating the capacity of each model trained on the data where for the same number of parameters the models show lower training error for $C_{l\,max}$ compared to $C_{d\,min}$. Increased error levels are observed for the range of very large Reynolds numbers (i.e. $9x10^6$ and above), which would be relevant especially to very large offshore wind turbines (10MW+). However, for most of the current onshore and offshore designs, current methodology gives acceptable prediction levels for $C_{l\,max}$ and $C_{d\,min}$, which could in turn be used in recently proposed Reynolds number extrapolation schemes in the literature[6, 7]. We also observe that the prediction performance is notably better for the two NACA test airfoils. This outcome is attributed to the fact that the majority of the database is constructed from NACA profiles. The error levels for the DU00-W-212 airfoil are somewhat higher for RF and DTE models and comparably better for the case of MLP. This discrepancy may be explained by the larger parameter space of the MLP model, allowing it to better fit the complexities of the underlying domain.

References

[1] N. Sezer-Uzol, O. Uzol, and E. Orbay-Akcengiz, “CFD Simulations for Airfoil Polars,” in *Handbook of Wind Energy Aerodynamics*, B. Stoevesandt, G. Schepers, P. Fuglsang, and Y. Sun, Eds., Cham: Springer International Publishing, 2022, pp. 303–329. doi: 10.1007/978-3-030-31307-4_12.

[2] O. Pires, X. Munduate, O. Ceyhan, M. Jacobs, J. Madsen, and J. G. Schepers, ‘Analysis of the high Reynolds number 2D tests on a wind turbine airfoil performed at two different wind tunnels’, Journal of Physics: Conference Series, vol. 749, no. 1, p. 012014, Sep. 2016.

[3] G. K. Yamauchi and W. Johnson, “Trends of Reynolds Number Effects on Two-Dimensional Airfoil Characteristics for Helicopter Rotor Analyses,” California, Apr. 1983. [Online]. Available: https://ntrs.nasa.gov/search.jsp?R=19830016201

[4] K. Pettersson and A. Rizzi, “Aerodynamic scaling to free flight conditions: Past and present,” *Progress in Aerospace Sciences*, vol. 44, no. 4, pp. 295–313, May 2008, doi: 10.1016/j.paerosci.2008.03.002.

[5] Ö. Ceyhan, “Towards 20 MW Wind Turbine: High Reynolds Number Effects on Rotor Design,” 2012. doi: https://doi.org/10.2514/6.2012-1157.

[6] A. C. Özgören and O. Uzol, “A Data-Driven Approach for the Prediction of Reynolds Number Effects on Wind Turbine Airfoil Aerodynamic Polars.” Authorea Preprints, 2023. doi: 10.22541/au.168873425.50156707/v1.

[7] A. C. Özgören, "Reynolds number extrapolation for wind turbine airfoil polars: a data-driven approach," Middle East Technical University, 2023. Accessed: Mar. 24, 2024. [Online]. Available: https://open.metu.edu.tr/handle/11511/102045
[8] R. Wallach, B. Mattos, R. Girardi, and M. Curvo, "Aerodynamic Coefficient Prediction of Transport Aircraft Using Neural Network," in *44th AIAA Aerospace Sciences Meeting and Exhibit*. doi: 10.2514/6.2006-658.
[9] C. Sabater, P. Stürmer, and P. Bekemeyer, "Fast Predictions of Aircraft Aerodynamics Using Deep-Learning Techniques," *AIAA Journal*, vol. 60, no. 9, pp. 5249–5261, 2022, doi: 10.2514/1.J061234.
[10] I. H. Abbott, A. E. Von Doenhoff, and L. S. Stivers, "NACA Report No. 824 - Summary of Airfoil Data," Jan. 1945.
[11] M. T. Akram and M.-H. Kim, "Aerodynamic Shape Optimization of NREL S809 Airfoil for Wind Turbine Blades Using Reynolds-Averaged Navier Stokes Model—Part II," *Applied Sciences*, vol. 11, no. 5, 2021, doi: 10.3390/app11052211.
[12] P. Della Vecchia, E. Daniele, and E. D'Amato, "An airfoil shape optimization technique coupling PARSEC parameterization and evolutionary algorithm," *Aerosp Sci Technol*, vol. 32, no. 1, pp. 103–110, Jan. 2014, doi: 10.1016/j.ast.2013.11.006.
[13] S. Ray, "A Quick Review of Machine Learning Algorithms," in *2019 International Conference on Machine Learning, Big Data, Cloud and Parallel Computing (COMITCon)*, 2019, pp. 35–39. doi: 10.1109/COMITCon.2019.8862451.
[14] C. Cortes and V. Vapnik, "Support-vector networks," *Mach Learn*, vol. 20, no. 3, pp. 273–297, 1995, doi: 10.1007/BF00994018.
[15] M. H. Sadraey, Aircraft design: A systems engineering approach. Chichester: John Wiley and Sons, 2013.
[16] O. Pires, X. Munduate, O. Ceyhan, M. Jacobs, and H. Snel, "Analysis of high Reynolds numbers effects on a wind turbine airfoil using 2D wind tunnel test data," in *Journal of Physics: Conference Series*, Institute of Physics Publishing, Oct. 2016. doi: 10.1088/1742-6596/753/2/022047.